



Research Article

Ultraviolet B Irradiation Alters the Level and miR Contents of Exosomes Released by Keratinocytes in Diabetic Condition

Jinju Wang^{1*} , Kartheek Pothana², Shuzhen Chen¹, Harshal Sawant¹, Jeffrey B. Travers^{2,3} , Ji Bihi¹ and Yanfang Chen²

¹Department of Biomedical Sciences, Joan C Edwards School of Medicine, Marshall University, Huntington, WV,

²Department of Pharmacology and Toxicology, Boonshoft School of Medicine, Wright State University, Dayton, OH,

³The Dayton V.A. Medical Center, Dayton, OH,

Received 6 October 2021, accepted 14 December 2021, DOI: 10.1111/php.13583

ABSTRACT

Ultraviolet B (UVB) stimulates the generation of extracellular vesicles, which elicit systemic effects. Here, we studied whether UVB affects the release and microRNA (miR) content of keratinocyte exosomes (EXs) in diabetic conditions. *In vitro*, we examined the UVB effects on affecting EX release from keratinocyte HaCaT cells (HaCaT-EX) pretreated with high glucose. HaCaT-EX functions were evaluated on Schwann cells (SCs). *In vivo*, UVB-induced miR change in skin EXs of diabetic db/db mice was analyzed. The miRs of interest were validated in HaCaT-EXs. We found that: (1) UVB promoted HaCaT-EX generation in dose- and time-dependent manners; 100 and 1800 J m⁻² of UVB had the most prominent effect and were selected as effective low- and high-fluence UVB *in vitro*. (2) A total of 13 miRs were differentially expressed >3-fold in skin EXs in UVB-treated db/db mice; miR-126 was the most up-regulated by low-fluence UVB. (3) Functional studies revealed that the SC viability was improved by low-fluence UVB HaCaT-EXs, while worsened by high-fluence UVB HaCaT-EXs. (4) MiR-126 inhibitor attenuated the effects induced by low-fluence UVB HaCaT-EXs. Our data have demonstrated that low- and high-fluence UVBs promote HaCaT-EX generation but differentially affect exosomal miR levels and functions under diabetic conditions.

INTRODUCTION

Diabetes mellitus is the most common endocrine disease that has a severe impact on health systems worldwide. Increased blood glucose causes damage to a wide range of cell types including keratinocytes and Schwann cells in the skin system (1). The skin represents the primary barrier protecting against pathogen invasion and excessive water loss, provides sensation and facilitates the production of vitamin D (2). It has been reported that skin

alterations can be found in about 30% of diabetes subjects and frequently occur before the diagnosis (3), and approximately 40% of diabetic patients are diagnosed with neuropathy. Diabetic neuropathy is characterized by progressive, distal-to-proximal degeneration of peripheral nerves that leads to pain, weakness and eventual loss of sensation (4). There is no effective treatment and controlling blood glucose and improving lifestyle only delay the onset and slow the progression.

Ultraviolet B (UVB) is a type of solar irradiation that has several known effects on skin health. Excess exposure to UVB could cause sunburn and skin cancer, while appropriate UVB irradiation could modulate the immune system such as through systemic anti-inflammatory effects (5). For example, Xue and colleagues have shown that appropriate exposure to UVB could promote cutaneous synthesis of the hormone-mediator vitamin D (6). Meanwhile, preclinical (7–9) and human studies (10–12) have demonstrated that ultraviolet irradiation could elicit beneficial effects on overall metabolic health. Studies have demonstrated that adult mice fed a high fat diet and exposed repeatedly to sub-erythemal (nonburning) UVB over 12 weeks gained less weight, exhibited reduced metabolic dysfunction and less hepatic steatosis and inflammation compared to that found in sham-treated mice (8,9). Exposure to UVB has also shown to suppress further weight gain and metabolic dysfunction in already “overweight” mice (7), suggesting that UVB might be effective when disease processes have already been underway. All these findings indicate that UVB might elicit favorable effects on diabetic complications.

Keratinocytes constitute >90% of the skin epidermal cells and UVB only reaches the epidermal layer of the skin. The beneficial effects of UVB might be related to mediators released from keratinocytes, although the underlying mechanism has not been addressed. Recently, there are growing interests of the role of extracellular vesicles in human diseases. Exosomes (EXs), a major type of extracellular vesicles, are emerging as a novel type of intercellular communicator (13). They are implicated in skin diseases and could serve as biomarkers in dermatology (14,15). EXs from human adipose-derived stem cells have been shown to promote proliferation and migration of skin fibroblasts (16). Our group has demonstrated that UVB irradiation that reaches the epidermis stimulates the release of microvesicle *in vitro* and *in vivo* (17,18). Of interest, studies have suggested that

*Corresponding author email: wangjin@marshall.edu (Jinju Wang)

© 2021 The Authors. *Photochemistry and Photobiology* published by Wiley Periodicals LLC on behalf of American Society for Photobiology

This is an open access article under the terms of the [Creative Commons Attribution-NonCommercial-NoDerivs](https://creativecommons.org/licenses/by-nc-nd/4.0/) License, which permits use and distribution in any medium, provided the original work is properly cited, the use is non-commercial and no modifications or adaptations are made.

keratinocyte EXs could participate in regulating cutaneous immunity and pigmentation (19–21). UV irradiation induces the release of keratinocyte EXs that communicate with melanocytes to regulate pigmentation (20,21). Extracellular microvesicles released by melanocytes after UV irradiation promote intercellular signaling in keratinocytes (22). Given that EXs could potentially serve a messenger function and UVB only reaches the epidermis, we speculated that keratinocyte EXs might be one mechanism by which UVB generates signals relevant to diabetes.

It has been documented that the cargoes carried by EXs such as nucleic acids, proteins and downstream functions of EXs are vastly different, depending on the cell origin and status (23,24). Increasing evidence indicate that microRNA (miRs) in extracellular vesicles including EXs play critical roles in their elicited effects. Qian and colleagues reported that miR-21 carried by keratinocyte microvesicles is implicated in fibroblast-mediated angiogenesis (25). Intriguingly, low- and high-fluences of UVB have been shown to elicit different effects on regulating cytokine expression (26,27). Given the content and function of EXs vary upon their generation condition, whether different doses of UVB might affect EX generation from keratinocytes and modulate the miR profiling in keratinocyte EXs and their function in hyperglycemia condition is of interest.

In this study, we aimed to test the hypothesis that low- and high-fluences of UVB differentially affect the release, miR profile and function of EXs released from keratinocytes in diabetic condition using both *in vitro* and *in vivo* models.

MATERIALS AND METHODS

Study of UVB on EX release in a diabetic skin cell model. Cell culture. HaCaT cells, a human keratinocyte cell line, were used in this study. HaCaT cells were cultured with complete medium consist of DMEM media (4.5 g L⁻¹ D-glucose) supplemented with 10% fetal bovine serum (FBS), 1% L-glutamine and 1% Pen-Strep antibiotic solution in a standard incubator (37°C, 5% CO₂). Culture media was replaced every two days. HaCaT cells were split at 1:7 ratios and passages 55–75 were used for this study. To generate a diabetic skin cell model, the HaCaT cells were grown in 10-cm dishes to reach 70–80% confluency, then the complete medium was replaced with high glucose (HG) medium that was consist of complete medium plus 25 mM of D-glucose and incubated for 24 h. On the next day, cells were used for different fluences of UVB irradiation stimulation. HaCaT cells cultured in normal condition were served as controls.

UVB irradiation to stimulate EXs release from HaCaT cells. On the treatment day, HaCaT cells cultured in HG or normal condition (NC) were washed with PBS for three times and then 3 mL of HBSS was added. Cells were then exposed for 0, 34, 68, 170, 306, 612 and 1224 s of UVB, corresponding to the low UVB fluences of (0, 50, 100, 200, 500) (28) and high UVB fluences (900, 1800, 3600 J m⁻²) (17) by using a Philips F20T12/UVB lamp. The intensity of the UVB source was measured before each experiment using an IL1700 radiometer and a SED240 UVB detector (International Light) at a distance of 8 cm from the UVB source to the cells. After UVB treatment, HBSS was removed, and 4 mL of serum-free culture medium was added to each dish. Then the cells were returned to the incubator for additional 4 or 24 h. The cell culture medium was collected at different time points (0, 4, 24 h) after the treatment. For the 24 h group, culture medium was entirely replaced with fresh serum-free medium after 4 h treatment to get rid of the particles released at the first 4 h. Experiments were independently repeated 6 times.

EX isolation from the cell medium of HaCaT cells. Cell medium at different time points was collected for EX isolation as we previously reported (29). In brief, the culture medium was collected and centrifuged at 300 g for 5 min followed by 2000 g for 20 min. The obtained supernatant was centrifuged at 20 000 g for 70 min, then the supernatant was ultra-centrifuged at 170 000 g for 90 min to pellet the EXs (29).

After ultracentrifugation, the supernatant was discarded, and the pellet was resuspended in 100 µL of sterile-filtered phosphate buffer saline (PBS) and used for RNA extraction or particle enumeration.

Nanoparticle tracking analysis (NTA). The size and concentration determination of the isolated EXs was carried out by the instrument NS300 (Nanosight, Amesbury, UK) as we reported (29). In brief, the EX-samples were diluted with sterile-filtered PBS to a concentration of 10⁷–10⁸ particles mL⁻¹. After diluting the sample, 700 µL of the same was loaded in the instrument for movement tracking at the rate of 30 frames s⁻¹. The videos with particle movement were recorded at least three times per sample at different positions which were analyzed by the NTA software (version 2.3, Nanosight). The NTA results were produced as a mean of three tests performed per sample and the particle concentration was calculated after considering the accurate dilution factor for the NTA results.

Animal study of UVB irradiation on the release and miR profiling of skin EXs in diabetic mice. Mice. Nine to ten-week-old type 2 diabetic db/db mice (female and male) and age-matched control db/c mice were purchased from the Jackson Laboratory. All mice were maintained in a 22°C room with a 12 h light/dark cycle and fed with standard chow and drinking water *ad libitum*. The body weights were recorded weekly. The ages of mice were 15–16 weeks at the time of experimentation. Nonfasting blood glucose level was measured prior to UVB irradiation. A drop of blood was obtained from the tail, and glucose concentrations were determined using Accu-Check Compact glucose test strips. All experimental procedures were approved by the Wright State University Laboratory Animal Care and Use Committee and were in accordance with the Guide for the Care and Use of Laboratory Animals issued by the National Institutes of Health.

UVB irradiation on mouse dorsal skin. The dorsal hairs of the mice were shaved using clippers one day before the experimentation. All mice were randomly divided into three groups (*n* = 4/group): non-UVB, low-UVB fluence (2500 J m⁻²), high-UVB fluence (7500 J m⁻²). UVB irradiation was applied for 0, 13 min 45 s and 41 min 15 s on the shaved dorsal skin, corresponding to the low-UVB (2500 J m⁻²) (30) and high-UVB (7500 J m⁻²) (18). UVB source was a Philips F20T12/UVB lamp. The intensity of the UVB source was measured before each experiment using an IL1700 radiometer and a SED240 UVB detector (International Light) (30). The mice were then returned to their home cages. Skin samples were collected 24 h after the treatment.

EX isolation from mice skin tissue biopsy samples. Twenty-four hours after UVB irradiation, mice were anesthetized by Ketamine/Xylazine (100 and 10 mg kg⁻¹, respectively) i.p. injection and the skin tissue biopsy were taken from the mice skin using 5-mm disposable biopsy punch. Skin EXs were isolated as we recently reported (18). In brief, the biopsied tissue was weighted, fat trimmed and then cut up finely in the microcentrifuge tube, digested in 0.5 mL of 5 mg mL⁻¹ collagenase and dispase solution made in deionized filtered water, and gently shaken overnight at 37°C. After overnight digestion, sample was spun at 2000 g for 20 min to remove tissue, then followed with 20 000 g for 10 min and 20 000 g for 70 min to remove remaining tissue, subcellular component and microvesicles. EXs were then pelleted by ultracentrifugation at 170 000 g for 90 min. EX pellet was resuspended in 100 µL of filtered PBS for NTA or stored in –80°C for miRNome profiling analysis.

MiR profiling analysis of EXs from mice skin biopsy tissues. The total RNAs of skin EXs isolated from different treatment groups were extracted by using the Trizol agent. RNA was eluted in 10 µL of RNase-free water. The concentration of RNA was measured by a Nanodrop 2000. The miR profiling of EXs isolated from db/db mice skin tissue biopsy samples was performed with the mouse miRNome microRNA Profilers QuantiMirTM (384-well plate) from System Biosciences (SBI, Mountain View, CA). The miR assay primers (709 primers) were resuspended prior to use. The QuantiMir RT kit was used to prepare cDNA from the eluted RNA by following the manufacture's instruction. A SYBR green-based qPCR was performed in the QuantStudio 7 Flex instrument: 50°C for 2 min, 95°C for 10 min, 95°C for 15 s, 60°C for 1 min (40 cycles), data read at 60°C for 1 min step. Three endogenous reference RNAs (U1, U6, RNU43) were used as normalization signals. The results of miRNome profiling of each pair were processed by array assays and the fold change >3 was shown. The qPCR array arrangement was downloaded from the SBI website and data was analyzed by 2^{-ΔΔC_T} method.

Quantitative RT-PCR analysis. To further validate the expressions of miRs of interest, qRT-PCR was conducted with HaCaT-EXs. Reverse

transcription (RT) reactions were performed using PrimeScript™ RT reagent kit (TaKaRa, San Jose, CA, Japan) and PCR reactions were conducted using SYBR Premix EX Taq™ II kit (TaKaRa). The primers used are listed in Table 1. The relative expression level of each gene was normalized to U6 and calculated using the $2^{-\Delta\Delta C_T}$ method. Experiments were independently repeated 4 times.

Functional study of UVB-induced EXs from keratinocytes. Co-culture of HaCaT-EXs with Schwann cells. Schwann cells (ATCC-CRL3387) were cultured using DMEM high glucose with 10% fetal bovine serum (FBS) and 1% L-glutamine and 1% Pen-Strep antibiotic solution in an incubator with maintaining 37°C and 5% CO₂ conditions. Schwann cells were split at 1:4 ratio. Culture media was replaced every two days. For co-culture experiment, Schwann cells were cultured to 60–70% confluency and treated with HG (25 mM) to mimic the diabetic condition for 48 h. Then the Schwann cells were divided into three co-culture groups: control (culture medium only), low-UVB fluence HaCaT-EXs (2×10^9 EXs mL⁻¹), high-UVB fluence HaCaT-EXs (2×10^9 EXs mL⁻¹). To block the effect of miR-126, some of Schwann cells were treated with miR-126 inhibitor (1 nM, Dharmacon, Lafayette, CO) that was mixed with DharmafECT transfection reagent (Dharmacon). The mixed solution was then added to the culture medium HaCaT-EXs (31). After 24 h co-culture, Schwann cells were collected for MTT cell viability assay.

Cell viability analysis of Schwann cells. Cell viability of Schwann cells after co-culture with different types of HaCaT-EXs was determined using 3-(4,5-dimethylthiazol-2-yl)-2,5-diphenyltetrazolium bromide (MTT). In brief, Schwann cells were cultured in 96 well plates at 100% confluency. Triplicates were maintained as per the

manufacturer's instructions. After the co-culture when Schwann cells were ready for assay, the media was replaced with 100 µL of fresh media, and to each of the wells, 10 µL of 12 mM MTT solution was added and mixed well, then incubated for 2 h. Later 85 µL of the media was discarded, leaving 25 µL in the wells. Fifty microlitre of DMSO was added, mixed by vigorous pipetting and incubated at 37°C for 10 min. The samples were mixed again, and absorbance was read at 540 nm under a microplate reader. Experiments were independently conducted triplicates.

Statistical analysis. Data was expressed as mean ± standard error. The paired comparison was analyzed using Student's *t*-test. The comparison of multiple groups was detected by one-way or two-way ANOVA with a Turkey or other appropriate *post hoc* test. Statistical calculations were performed with GraphPad Prism 9 (San Diego, CA). *P* < 0.05 was considered statistically significant.

RESULTS

UVB promotes EX release from HaCaT cells in dose- and time-dependent manners, with an augmented effect in HG condition

To determine the dose effects of UVB irradiation on EX release from epidermal cells, HaCaT cells cultured in NC or HG condition were exposed to different fluences of UVB irradiation. After incubation in serum-free media for additional 24 h, EXs were

Table 1. Primer sequence for miRs used for qRT-PCR.

hsa-miR-23a
RT primer: 5'-GTCGTATCCAGTGCAGGGTCCGAGGTATTCGACTGGATACGACAATCCC -3'
F primer: 5'- AAATTTGGGGTTCTCTGGGGATGG -3'
hsa-miR-29a
RT primer: 5'- GTCGTATCCAGTGCAGGGTCCGAGGTATTCGACTGGATACGACCTGAAC -3'
F primer: 5'- GGGCGCACTGATTTCTTTTGGTG-3'
hsa-miR-31
RT primer: 5'- GTCGTATCCAGTGCAGGGTCCGAGGTATTCGACTGGATACGACAGCTAT -3'
F primer: 5'- GCGATTAGGCAAGATGCTGGCAT-3'
hsa-miR-125a
RT primer: 5'- GTCGTATCCAGTGCAGGGTCCGAGGTATTCGACTGGATACGACTCACAG-3'
F primer: 5'- GGCCACTCCCTGAGACCCCTTTAA-3'
hsa-miR-126a-5p
RT primer: 5'- GTCGTATCCAGTGCAGGGTCCGAGGTATTCGACTGGATACGACCCGCGTA-3'
F primer: 5'- GCGGGGCATTATTACTTTTGGTA -3'
hsa-miR-146a
RT primer: 5'- GTCGTATCCAGTGCAGGGTCCGAGGTATTCGACTGGATACGACAACCCA-3'
F primer: 5'- GGGCCCTGAGAAGTGAATTCAT-3'
hsa-miR-155
RT primer: 5'-GTCGTATCCAGTGCAGGGTCCGAGGTATTCGACTGGATACGACACC CCT-3'
F primer: 5'- GGGGGGGCTTAATGCTAATTGTGAT -3'
hsa-miR-181a
RT primer: 5'- GTCGTATCCAGTGCAGGGTCCGAGGTATTCGACTGGATACGACTCAC-3'
F primer: 5'- CGCGGTAACATTCAACGCTGTCCG-3'
hsa-miR-196a
RT primer: 5'- GTCGTATCCAGTGCAGGGTCCGAGGTATTCGACTGGATACGACCCCAAC-3'
F primer: 5'- GCGCGCTAGGTAGTTTCATGTTG-3'
hsa-miR-199a
RT primer: 5'- GTCGTATCCAGTGCAGGGTCCGAGGTATTCGACTGGATACGACGAACAG-3'
F primer: 5'- GGCAACCCAGTGTTCAGACTAC-3'
hsa-miR-221
RT primer: 5'- GTCGTATCCAGTGCAGGGTCCGAGGTATTCGACTGGATACGACAAATCT-3'
F primer: 5'- GGAGCCACTGGCATAACAATGTA-3'
hsa-miR-222
RT primer: 5'-GTCGTATCCAGTGCAGGGTCCGAGGTATTCGACTGGATACGACAGGATC-3'
F primer: 5'- AACCGCTCAGTAGCCAGTGTAG-3'
hsa-miR-411
RT primer: 5'- GTCGTATCCAGTGCAGGGTCCGAGGTATTCGACTGGATACGACCGTACG -3'
F primer: 5'- CCCGGTAGTAGACCGTATAGCG -3'
R primer for all miRs: 5'- CCAGTGCAGGGTCCGAGGTA -3'
U6 F primer: 5'- CTCGCTTCGGCAGCACCA -3'; R primer: 5'- AACGCTTCACGAATTTGCGT-3'

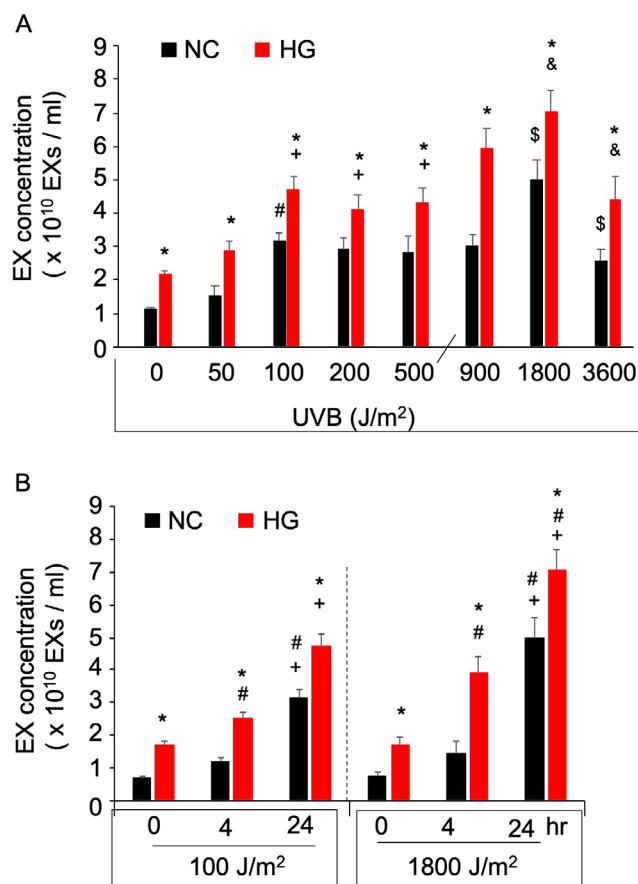


Figure 1. UVB irradiation promotes EX release from HaCaT cells in dose- and time-dependent manners. The HaCaT cells were cultured in NC or HG condition and then exposed to different fluences of UVB. (A) Summarized data showing the concentration of EXs released from HaCaT cells stimulated by different fluences of UVB. * $P < 0.05$ vs NC at the same UVB irradiation; $^{\#}P < 0.05$ vs 200 or 500 in NC; $^{+}P < 0.05$ vs 0 or 50 in HG; $^{\$}P < 0.05$ vs 900 in NC; $^{\&}P < 0.05$ vs 900 or 3600 in HG. (B) The summarized data show the concentration of HaCaT-EXs in different time points after UVB irradiation. * $P < 0.05$ vs NC at the same time point; $^{\#}P < 0.05$ vs 0 h at the same UVB fluence; $^{+}P < 0.05$ vs 0 or 4 h at the same UVB fluence. Data are expressed as mean \pm SD. $N = 6$ /group.

collected from the culture media and the concentration was analyzed by NTA. As shown in Fig. 1A, for the HaCaT cells growing in normal glucose condition, 50 J m⁻² UVB irradiation did not significantly affect EX secretion as compared to the cells without UVB exposure, whereas 100, 200 or 500 J m⁻² UVB irradiation significantly increased the release of EXs, of which there was no significant difference among the three groups. Regarding the high-UVB fluence groups, 1800 J m⁻² UVB irradiation induced the highest generation of EXs as compared to 900 or 3600 J m⁻² did.

When the cells were grown in HG condition, 50 J m⁻² UVB promoted EX generation, suggesting that the cells in HG condition might be more sensitive to UVB irradiation. 100, 200 or 500 J m⁻² UVB significantly stimulated the release of EXs, with a peak at 100 J m⁻² UVB. Among the high-UVB fluence groups, 1800 J m⁻² UVB elicited the greatest release of EXs. Of note, with the same UVB, HaCaT cells in HG condition released

more EXs than the cells in NC did. All these data indicate that UVB promoted EX release from HaCaT cells in a dose-dependent manner. Based on these findings, we chose 100 and 1800 J m⁻² to represent an effective low- and high- UVB irradiation for the subsequent studies generating HaCaT-EXs.

Our previous study has demonstrated that UVB treatment of HaCaT cells could result in an increased level of microvesicle generation at 4 h (17). Here, we studied whether the effect elicited by low- and high- fluences of UVB on EX release from HaCaT cells under HG condition was in a time-dependent manner. After serum-free media incubation for 0, 4 or 24 h, EXs were collected and enumerated by NTA. As shown in Fig. 1B, in response to both UVB fluences, the level of EXs at 24 h were much higher than those measured at 0 or 4 h post-UVB irradiation.

UVB alters the level and miR profiling of skin EXs in T2D diabetic mice

To determine the effect of UVB irradiation on skin EX generation in diabetes, we treated the diabetic db/db and control db/c mice with either low- or high-fluence of UVB. Skin biopsy tissues were collected 24 h after the irradiation and used for EX isolation.

At the time of study, db/db mice weighed 44 ± 4 g compared with 28 ± 1.6 g of db/c mice, and the nonfasted blood glucose concentrations leveled in db/db at 520 ± 10 and in db/c at 104 ± 5 mg dL⁻¹. The isolated skin EXs positively expressed exosomal marker CD63 and keratinocyte-specific marker cytokeratin 14 (Fig. 2A). As revealed by the NTA analysis, baseline levels of skin EXs were increased in diabetic db/db mice than that in the control db/c mice (Fig. 2B). In response to irradiation with a low fluence of UVB (2500 J m⁻²), db/c mice had a slight increase of skin EXs, while db/db mice had a significant increase of EX generation. In response to a higher fluence of UVB (7500 J m⁻²) irradiation, the level of EXs in skin tissues was increased in both genotypes, but the db/db mice had a much higher level than that in the db/c mice. These data suggest that the diabetic mice skin is more sensitive to this UVB irradiation regime than control mice did. We then focused on investigating whether UVB irradiation affects miR contents of skin EXs. We conducted miRNome profiling analysis with the skin EXs from db/db mice.

As shown in Fig. 2C, there were seven differentially expressed miRs among 709 miRs when compared with the EXs from low-fluence UVB-irradiated db/db mice with db/db mice without UVB irradiation. The expression difference was >3-fold. Among them, two miRs (miR-155 and miR-199a-3p) were down-regulated and five miRs (miR-23a, miR-126-5p, miR-181a, miR-221 and miR-222) were up-regulated. There were eight differentially expressed miRs (>3-fold) when compared the EXs from high-fluence UVB-irradiated db/db mice with the sham-irradiated db/db mice, of which five miRs (miR-31, miR-125a, miR-126-5p, miR-196a, miR-222) were down-regulated and three miRs (miR-29a, miR-146a, miR-411) were up-regulated. As shown in the Venn diagram (Fig. 2D), two of these miRs (miR-126-5p and miR-222) were modulated by both low- and high- UVB irradiation. MiR-126 expression exhibited the greatest change in response to low-fluence UVB.

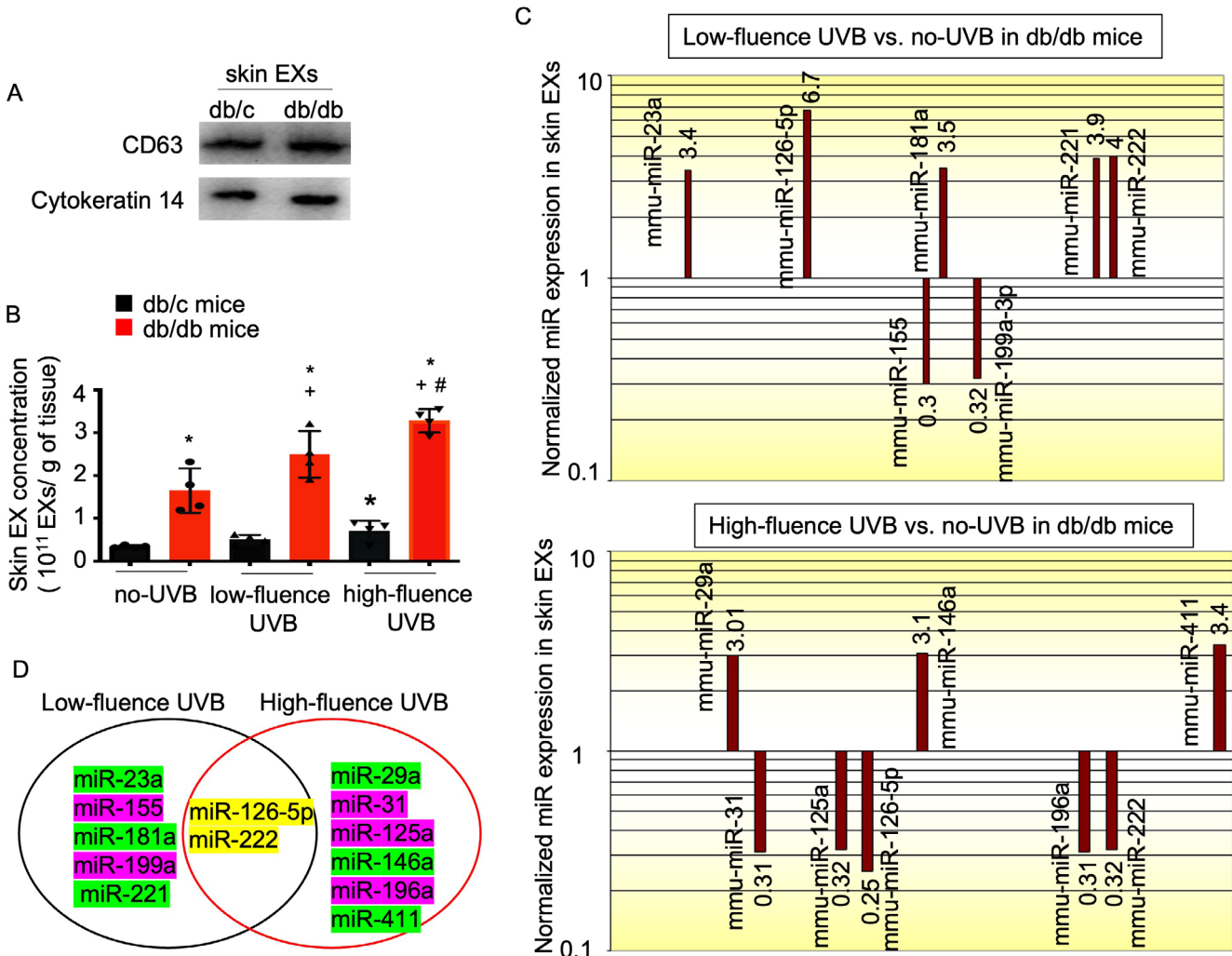


Figure 2. MiRNome analysis of miR expression profile in the skin EXs of db/db mice. (A) representative western blot bands of skin EXs expressing CD63 and cytokeratin 14. (B) summarized data showing the level of skin EXs in the two mouse groups. **P* < 0.05 vs db/c at the same UVB fluence; +*P* < 0.05 vs db/db no-UVB; #*P* < 0.05 vs db/db low-fluence UVB. Data are expressed as mean ± SD. *N* = 4/group. (B) The representative miR profiling graph showing the changes of miRs in skin EXs from db/db mice received low- or high- fluence UVB. (C) Venn diagram shows the miR changes in the skin EXs. Green: up-regulated miRs >3-fold; Pink: down-regulated miRs >3-fold; Yellow: up- or down- regulated in both groups.

Validation of the expressions of miRs in HaCaT-EXs: miR-126 expression is up-regulated in HaCaT-EXs generated in response to HG plus low-fluence UVB irradiation but decreased in response to HG plus high-fluence UVB

We further validated the relative levels of the 13 miRs screened by the miRNome profiling analysis in the EXs isolated from HaCaT cells in different NC or HG groups: no UVB, HG + low-fluence (100 J m⁻²) UVB, HG + high-fluence (1800 J m⁻²) UVB. The data show that (Fig. 3) the basal levels of three miRs (miR-29a, miR-155 and miR-199a) were upregulated, while nine miRs (miR-31, miR-125a, miR-126-5p, miR-146a, miR-181a, miR-196a, miR-221) were downregulated in HG HaCaT-EXs as compared to those in the NC HaCaT-EXs. Low-fluence UVB partially restored some of the down-regulated miRs (miR-23a, miR-29a, miR-31, miR-125a, miR-126-5p, miR-181a, miR-196a, miR-221 and miR-222) in HG HaCaT-EXs. Meanwhile, the data showed that high-fluence UVB could significantly up-regulate some miRs such as miR-29a, miR-146a, miR-155, miR-199a and miR-411 in HG HaCaT-EXs. The levels of miR-29a and miR-

155 in NC HaCaT-EXs were also raised by high-fluence UVB. Among the differently expressed miRs, miR-126-5p level change was the most in HaCaT-EXs generated under HG plus low-fluence UVB, or HG plus high-fluence (0.55 ± 0.09, 7.28 ± 1.06, 0.32 ± 0.07 for miR-126 level in HaCaT-EXs generated under HG, HG plus low-fluence UVB or HG plus high-fluence UVB, respectively).

HaCaT-EXs generated in response to HG plus low-fluence UVB improves Schwann cell viability via conveying miR-126

Since miR-126 level was remarkably altered in HaCaT-EXs by UVB irradiation, to illustrate whether these EXs can convey miR-126 to recipient cells, we conducted a co-culture study with Schwann cells and analyzed the miR-126 level in Schwann cells after co-culture. Our data showed that (Fig. 4A) HG-treated Schwann cells had a lower level of miR-126 than that seen in naïve Schwann cells. In contrast, co-culture with HaCaT-EXs released under NC plus 100 J m⁻² UVB irradiation had raised miR-126 level in Schwann cells. Of note, co-culture with HaCaT-EXs

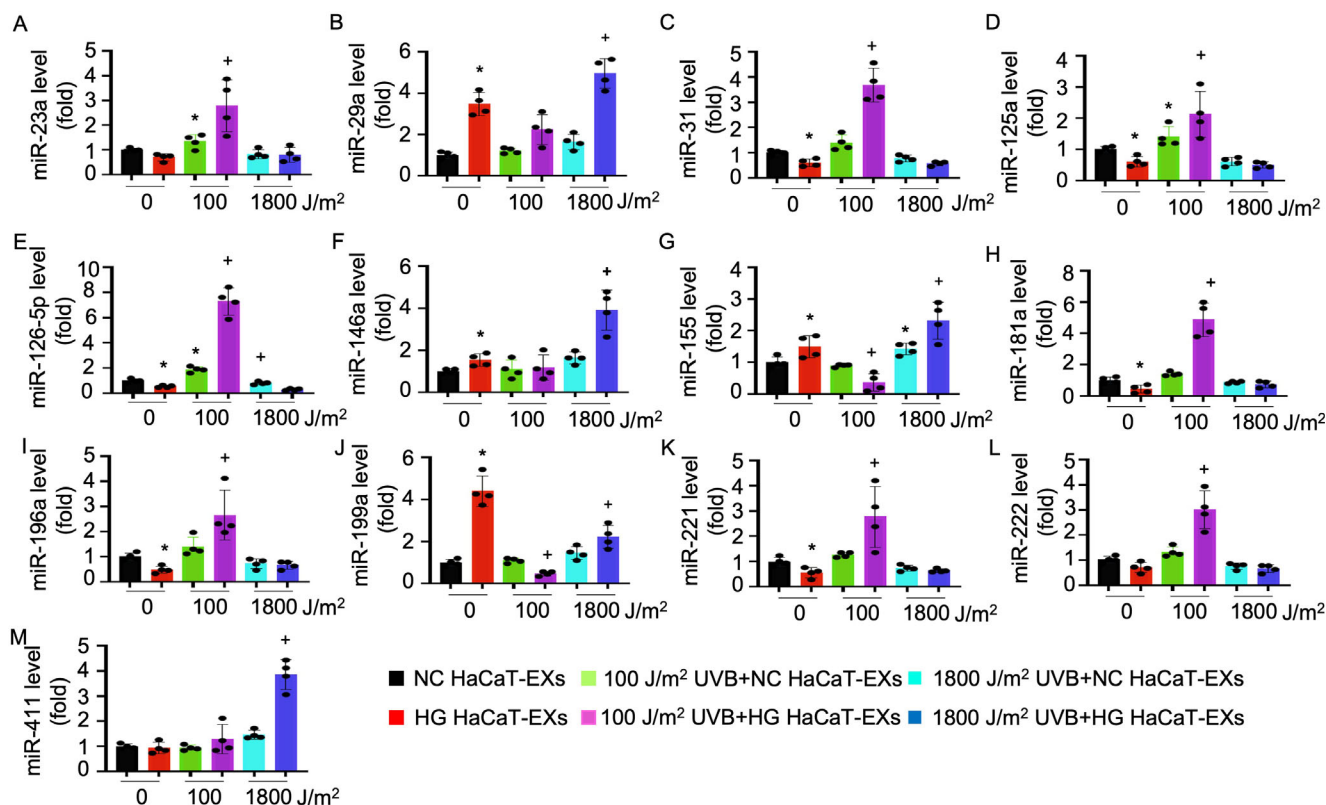


Figure 3. QRT-PCR analysis of miR expression in HaCaT-EXs. (A–M) miR expression levels in NC and HG HaCaT-EXs released in response to low- or high- fluence UVB. * $P < 0.05$ vs NC HaCaT-EXs; + $P < 0.05$ vs HG HaCaT-EXs or NC HaCaT-EXs at the same UVB fluence. Data are expressed as mean \pm SD. $N = 4$ /group. NC HaCaT-EXs: EXs generated from NC HaCaT cells; HG HaCaT-EXs: EXs generated from HG-treated HaCaT cells; 100 $J m^{-2}$ UVB+NC HaCaT-EXs: EXs generated from NC HaCaT cells exposed to 100 $J m^{-2}$ UVB; 100 $J m^{-2}$ UVB+HG HaCaT-EXs: EXs generated from HaCaT cells treated with HG plus 100 $J m^{-2}$ UVB; 1800 $J m^{-2}$ UVB+NC HaCaT-EXs: EXs generated from NC HaCaT cells treated with 1800 $J m^{-2}$; 1800 $J m^{-2}$ UVB+HG HaCaT-EXs: EXs generated from HaCaT cells treated with HG plus 1800 $J m^{-2}$ UVB.

released under HG plus 100 $J m^{-2}$ UVB irradiation significantly increased miR-126 level in Schwann cells. Not surprisingly, those EXs released in response to 1800 $J m^{-2}$ UVB irradiation did not significantly change miR-126 expression in Schwann cells.

To further determine whether UVB irradiation affects the function of HaCaT-EXs, we analyzed the cell viability of Schwann cells. Prior to being co-cultured, Schwann cells were treated with HG to mimic the diabetic condition *in vitro*. Our data (Fig. 4B) showed that the HaCaT-EXs released under NC plus 100 $J m^{-2}$ UVB irradiation slightly improved the cell viability of Schwann cells, but those released in response to NC plus 1800 $J m^{-2}$ UVB decreased the cell viability of Schwann cells. As expected, HaCaT-EXs generated under HG plus 100 $J m^{-2}$ UVB irradiation significantly improved the cell viability of HG-injured Schwann cells, whereas HaCaT-EXs generated from HG plus 1800 $J m^{-2}$ UVB irradiation further decreased the Schwann cell viability. Meanwhile, our data showed that miR-126 inhibitor could block the effect of HaCaT-EXs released under NC or HG plus 100 $J m^{-2}$ UVB irradiation. These results suggest that miR-126 is implicated in the effects on Schwann cells elicited by HaCaT-EXs.

DISCUSSION

In this study, we have demonstrated that UVB irradiation can promote the release of EXs from keratinocytes, especially in high

glucose mimicking the diabetic condition. We also have shown that this effect is dose- and time-dependent. Moreover, we identified that low- and high- fluences of UVB could alter the miR profiling of skin EXs *in vivo* and *in vitro*. Loss-of function studies confirmed that miR-126 might be responsible for the effects on Schwann cells elicited by HaCaT-EXs, suggesting that UVB might have effects on Schwann cells through UVB-induced release of EXs from keratinocytes.

Keratinocytes are the most abundant cell type in the skin and spatially occupy the most basal and superficial layers of the stratified epithelia, serving as the primary barrier between the body's interior and the external environment. UVB has multiple positive effects to include the promotion of Vitamin D synthesis (6) and elicitation of favorable effects on metabolic disease (7). Phototherapy of UVB has been applied as a common phototherapy treatment for skin disorders such as atopic dermatitis and psoriasis (32,33). UVB only reaches the epidermal layer of the skin. Increasing evidence shows that keratinocyte-released extracellular vesicles including EXs play an important role in skin tissue intercellular communication and are associated with several different types of human skin alterations (20,25). Our group has demonstrated that UVB phototherapy could increase microvesicle generation in the circulation at 4 h post-UVB (17). Given that EX level and cargoes vary upon the stimulation condition of the parent cells (13), we speculate that the level and cargoes of EXs released by keratinocytes under different fluences of UVB stimuli are altered. To test our hypothesis, we first determined different

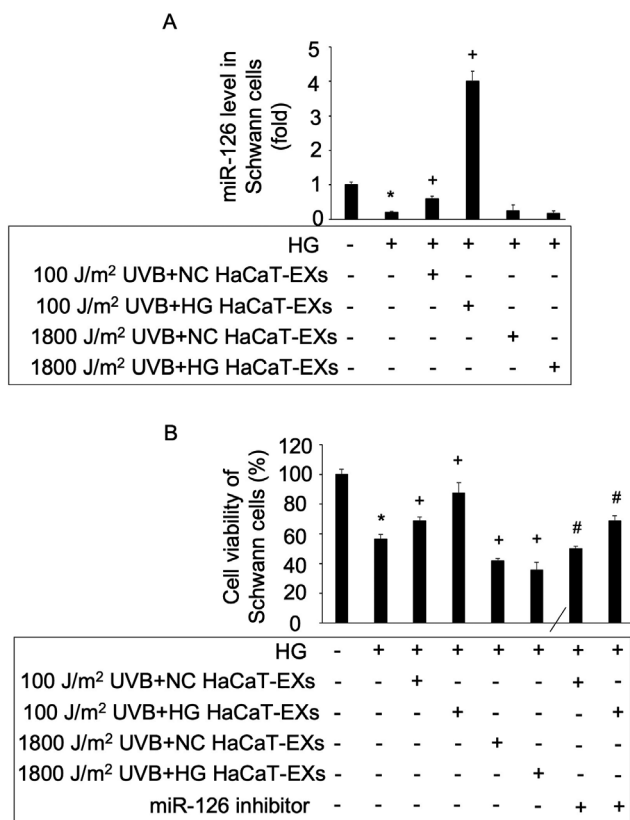


Figure 4. HaCaT-EXs co-culture altered the viability of Schwann cells. EXs were collected from the culture medium of HaCaT cells exposed to NC or HG plus low- or high- fluence UVB and used for co-culture assay. The concentration of EXs was 2×10^9 EXs mL⁻¹. Schwann cells were exposed to HG 48 h prior to the co-culture. MTT assay was conducted at 24-h co-culture to evaluate the cellular viability of Schwann cells, and qRT-PCR was applied to determine miR-126 level in Schwann cells after EX co-culture. (A) miR-126 level in Schwann cells co-cultured with different types of EXs. (B) Schwann cell viability in different co-culture groups. * $P < 0.05$ vs control; + $P < 0.05$ vs HG only; # $P < 0.05$ vs 100 J m⁻² UVB + NC HaCaT-EXs or 100 J m⁻² UVB + HG HaCaT-EXs. Data are expressed as mean \pm SD. $N = 3$ /group.

fluences of UVB on keratinocyte EXs in the cell-culture system. Our data revealed that both low- and high-fluence UVB stimulated EXs generation. This effect was much more pronounced when the HaCaT cells were cultured under HG condition, suggesting that the hyperglycemia environment makes the keratinocyte to be more sensitive to UVB irradiation. Of note, our data revealed that among the low-fluence UVB ranges, 100 J m⁻² elicited the greatest effects on stimulating EX release. This is in line with a previous study showing that low fluences of UVB do not result in growth retardation in HaCaT cells (34). Meanwhile, a relatively high-fluence UVB (1800 J m⁻²) stimulated the greatest generation of EXs from HaCaT cells in HG condition at 24-h post-UVB. Given that the function of EXs varies upon their release condition, besides the observed level change, we speculate that the EXs released under different fluences of UVB stimuli might carry varied cargoes that contribute to their functional effects.

In this study, we focused on the miRNAs contents of EXs, since increasing evidence indicate that the exosomal shuttled miRNAs play an important role in the keratinocyte extracellular vesicles mediated intercellular communication in the skin (20,25). Studies

from EXs isolated from the skin biopsy tissues of T2D diabetic mice in response to either low- or high-fluence UVB stimulation revealed two major findings. First, the diabetic db/db mice were more sensitive to UVB radiation to release EXs than the control mice did. This is consistent with the data observed in our *in vitro* cell model. Second, the miRNome profiling analysis was used to analyze the miR changes in EXs. The UVB fluences employed for these *in vitro* and *in vivo* studies were chosen based on previous and our recent study (18,30). We found 13 miRNAs were differently expressed >3-fold among 709 miRNAs in the diabetic skin-EXs at 24-h post-UVB irradiation. Some of these miRNAs are related to the pathogenesis of diabetic phenotype (miR-29a, miR-181a) (35,36) or have diabetic implications such as diabetic neuropathy (miR-199a) (37), some are associated with diabetic dermopathy (miR-155) (38) or diabetic angiopathy (miR-21, miR-126-5p) (25). The expressions of these miRNAs were validated in HaCaT-EXs which are in consistent with the data of miRNome.

It is well known that miR-126 plays critical roles in angiogenesis and maintenance of vascular integrity (39) and wound healing (40). However, in diabetes, its level is decreased in the circulation. We have demonstrated that the miR-126 carried by circulating endothelial progenitor cells microvesicles is responsible for the compromised function of endothelial progenitor cells in diabetes (41). Increasing evidence indicates that miR-126 plays an important role in the diabetic vascular complications. Some reports have shown that diabetic microangiopathy, including diabetic wounds, obtain a better curative effect via increasing the expression of miR-126 directly or indirectly (42,43). In this study, our data revealed that the miR-126 level was largely reduced in the skin-EXs of T2D db/db mice and HaCaT-EXs released under HG and low- fluences of UVB. Since the level of miR-126 differs substantially in EXs released under low- or high- fluence of UVB radiation, we hypothesized that miR-126 might affect the function of those EXs. Indeed, our data of the co-culture study findings have uncovered that HaCaT-EXs carrying a higher level of miR-126 exhibited different effects on Schwann cells as compared to those EXs which carried a relative low level of miR-126 did. With the miR-126 inhibitor manipulation, we found that the favorable effect elicited by HaCaT-EXs generated by HG plus low-fluence UVB radiation was abolished. These results therefore argue that the altered miR-126 level might be responsible for the effects of HaCaT-EXs on Schwann cells. Nevertheless, whether similar responses could be elicited by EXs released from primary keratinocytes that exposed to low- and high-fluence UVB radiation are waiting to be confirmed. Whether the changed miR-126 level in keratinocyte EXs contribute to the overall function of keratinocyte EX and thereby affect cutaneous damage in diabetes also require further investigation. In addition, the molecules that are responsible for the adverse effect exhibited by HaCaT-EXs generated in response to HG plus high-fluence UVB radiation on Schwann cells and the underlying mechanism of how UVB radiation affect miR packaging into EXs remain to be determined.

CONCLUSION

In summary, our data suggest that UVB alters the level and miRNAs contents of EXs released by keratinocytes under diabetic conditions. The level of miR-126 was significantly up-regulated by low-fluence of UVB yet down-regulated by higher UVB fluence,

suggesting that miR-126 in keratinocyte EXs might be involved in diabetic complications such as diabetic angiopathy and neuropathy.

Acknowledgements—This research was supported in part by grants from the National Institute of Arthritis and Musculoskeletal and Skin Diseases R21 AR071110 (to JB), the National Institutes of Health R01 HL062996 (to JBT), R01 ES031087 (to JBT and YC) and U.S. Veteran's Administration Merit Award 5I01BX000853 (to JBT). The contents of this manuscript do not represent the views of the Department of Veterans Affairs or the United States Government.

CONFLICT OF INTEREST

None.

AUTHOR CONTRIBUTION

JW, YC and JB conceived and designed this study; KP, SC, HS and JW performed the experiments; JW, JB and YC interpreted the data; JW and JB drafted the manuscript; JW, YC, JB and JBT revised the manuscript. All authors have given their final approval for this version of the paper to be published.

DATA AVAILABILITY STATEMENT

The datasets generated during this study are available from the corresponding author upon reasonable request.

REFERENCES

- Hulse, R. P., N. Beazley-Long, N. Ved, S. M. Bestall, H. Riaz, P. Singhal, K. Hofer, S. Harper, D. Bates and L. Donaldson (2015) Vascular endothelial growth factor- α 165b prevents diabetic neuropathic pain and sensory neuronal degeneration. *Clin. Sci. (lond)* **129**, 741–756.
- Baroni, A., E. Buommino, V. De Gregorio, E. Ruocco, V. Ruocco and R. Wolf (2012) Structure and function of the epidermis related to barrier properties. *Clin. Dermatol.* **30**, 257–262.
- Lima, A. L., T. Illing, S. Schliemann and P. Elsner (2017) Cutaneous manifestations of diabetes mellitus: A review. *Am. J. Clin. Dermatol.* **18**, 541–553.
- Pop-Busui, R., A. J. Boulton, E. L. Feldman, V. Bril, R. Freeman, R. A. Malik, J. Sosenko and D. Ziegler (2017) Diabetic neuropathy: A position statement by the American diabetes association. *Diabetes Care* **40**, 136–154.
- Hart, P. H., S. Gorman and J. J. Finlay-Jones (2011) Modulation of the immune system by UV radiation: More than just the effects of vitamin D? *Nat. Rev. Immunol.* **11**, 584–596.
- Xue, Y., L. Ying, R. L. Horst, G. Watson and D. Goltzman (2015) Androgens attenuate vitamin D production induced by UVB irradiation of the skin of male mice by an enzymatic mechanism. *J. Invest. Dermatol.* **135**, 3125–3132.
- Fleury, N., M. Feelisch, P. H. Hart, R. B. Weller, J. Smoothy, V. B. Matthews and S. Gorman (2017) Sub-erythral ultraviolet radiation reduces metabolic dysfunction in already overweight mice. *J. Endocrinol.* **233**, 81–92.
- Geldenhuis, S., P. H. Hart, R. Endersby, P. Jacoby, M. Feelisch, R. B. Weller, V. Matthews and S. Gorman (2014) Ultraviolet radiation suppresses obesity and symptoms of metabolic syndrome independently of vitamin D in mice fed a high-fat diet. *Diabetes* **63**, 3759–3769.
- Teng, S., L. Chakravorty, N. Fleury and S. Gorman (2019) Regular exposure to non-burning ultraviolet radiation reduces signs of non-alcoholic fatty liver disease in mature adult mice fed a high fat diet: Results of a pilot study. *BMC Res. Notes* **12**, 78.
- Fleury, N., S. Geldenhuis and S. Gorman (2016) Sun exposure and its effects on human health: Mechanisms through which sun exposure could reduce the risk of developing obesity and cardiometabolic dysfunction. *Int. J. Environ. Res. Public Health* **13**, 999.
- Gorman, S., R. M. Lucas, A. Allen-Hall, N. Fleury and M. Feelisch (2017) Ultraviolet radiation, vitamin D and the development of obesity, metabolic syndrome and type-2 diabetes. *Photochem. Photobiol. Sci.* **16**, 362–373.
- Shore-Lorenti, C., S. L. Brennan, K. M. Sanders, R. E. Neale, R. M. Lucas and P. R. Ebeling (2014) Shining the light on sunshine: A systematic review of the influence of sun exposure on type 2 diabetes mellitus-related outcomes. *Clin. Endocrinol. (oxf)* **81**, 799–811.
- Cocozza, F., E. Grisard, L. Martin-Jaular, M. Mathieu and C. Thery (2020) Snapshot: extracellular vesicles. *Cell* **182**, 262–262.e1.
- McBride, J. D., L. Rodriguez-Menocal and E. V. Badiavas (2017) Extracellular vesicles as biomarkers and therapeutics in dermatology: a focus on exosomes. *J. Invest. Dermatol.* **137**, 1622–1629.
- Wang, W. M., C. Wu and H. Z. Jin (2019) Exosomes in chronic inflammatory skin diseases and skin tumors. *Exp. Dermatol.* **28**, 213–218.
- Choi, E. W., M. K. Seo, E. Y. Woo, S. H. Kim, E. J. Park and S. Kim (2018) Exosomes from human adipose-derived stem cells promote proliferation and migration of skin fibroblasts. *Exp. Dermatol.* **27**, 1170–1172.
- Bihl, J. C., C. M. Rapp, Y. Chen and J. B. Travers (2016) Uvb generates microvesicle particle release in part due to platelet-activating factor signaling. *Photochem. Photobiol.* **92**, 503–506.
- Liu, L., A. A. Awoyemi, K. E. Fahy, P. Thapa, C. Borchers, B. Y. Wu, C. McGlone, B. Schmeusser, Z. Sattouf, C. Rohan, A. Williams, E. Cates, C. Knisely, L. Kelly, J. Bihl, D. Cool, R. Sahu, J. Wang, Y. Chen, C. M. Rapp, M. G. Kemp, R. M. Johnson and J. B. Travers (2021) Keratinocyte-derived microvesicle particles mediate ultraviolet b radiation induced systemic immunosuppression. *J. Clin. Invest.* **131**(10), e144963.
- Kotzerke, K., M. Mempel, T. Aung, G. G. Wulf, H. Urlaub, D. Wenzel, M. Schön and A. Braun (2013) Immunostimulatory activity of murine keratinocyte-derived exosomes. *Exp. Dermatol.* **22**, 650–655.
- Lo Cicero, A., C. Delevoye, F. Gilles-Marsens, D. Loew, F. Dingli, C. Guere, N. André, K. Vié, G. Niel and G. Raposo (2015) Exosomes released by keratinocytes modulate melanocyte pigmentation. *Nat. Commun.* **6**, 7506.
- Liu, Y., L. Xue, H. Gao, L. Chang, X. Yu, Z. Zhu, X. He, J. Geng, Y. Dong, H. Li, L. Zhang and H. Wang (2019) Exosomal miRNA derived from keratinocytes regulates pigmentation in melanocytes. *J. Dermatol. Sci.* **93**, 159–167.
- Waster, P., I. Eriksson, L. Vainikka and K. Ollinger (2020) Extracellular vesicles released by melanocytes after UVA irradiation promote intercellular signaling via mir21. *Pigment Cell Melanoma Res.* **33**, 542–555.
- Zhang, Y., Y. Liu, H. Liu and W. H. Tang (2019) Exosomes: Biogenesis, biologic function and clinical potential. *Cell Biosci.* **9**, 19.
- Kalluri, R. and V. S. LeBleu (2020) The biology, function, and biomedical applications of exosomes. *Science* **367**, eaau6977.
- Li, Q., H. Zhao, W. Chen, P. Huang and J. Bi (2019) Human keratinocyte-derived microvesicle miRNA-21 promotes skin wound healing in diabetic rats through facilitating fibroblast function and angiogenesis. *Int. J. Biochem. Cell Biol.* **114**, 105570.
- Liao, Y., J. Feng, Y. Zhang, L. Tang and S. Wu (2017) The mechanism of CIRP in inhibition of keratinocytes growth arrest and apoptosis following low dose UVB radiation. *Mol. Carcinog.* **56**, 1554–1569.
- Yarosh, D., D. Both, J. Kibitel, C. Anderson, C. Elmetts, D. Brash and D. Brown (2000) Regulation of TNF alpha production and release in human and mouse keratinocytes and mouse skin after UVB irradiation. *Photodermatol. Photoimmunol. Photomed.* **16**, 263–270.
- Chang, R. - S., C. - S. Chen, C. - L. Huang, C. - T. Chang, Y. Cui, W. - J. Chung, W. - Y. Shu, C. - S. Chiang, C. - Y. Chuang and I. - C. Hsu (2018) Unexpected dose response of HaCaT to UVB irradiation. *In Vitro Cell. Dev. Biol. Anim.* **54**, 589–599.
- Wang, J., R. Guo, Y. Yang, B. Jacobs, S. Chen, I. Wuchukwu, K. Gaines, Y. Chen, R. Simman, G. Lv, K. Wu and J. Bihl (2016) The

- novel methods for analysis of exosomes released from endothelial cells and endothelial progenitor cells. *Stem Cells Int.* **2016**, 2639728.
30. Travers, J. B., J. Weyerbacher, J. A. Ocana, C. Borchers, C. M. Rapp and R. P. Sahu (2019) Acute ethanol exposure augments low-dose UVB-mediated systemic immunosuppression via enhanced production of platelet-activating factor receptor agonists. *J. Invest. Dermatol.* **139**, 1619–1622.
 31. Ma, C., J. Wang, H. Liu, Y. Chen, X. Ma, S. Chen, Y. Chen, J. Bihl and Y. Yang (2018) Moderate exercise enhances endothelial progenitor cell exosomes release and function. *Med. Sci. Sports Exerc.* **50**, 2024–2032.
 32. Mehta, D. and H. W. Lim (2016) Ultraviolet b phototherapy for psoriasis: Review of practical guidelines. *Am. J. Clin. Dermatol.* **17**, 125–133.
 33. Jo, S. J., H. H. Kwon, M. R. Choi and J. I. Youn (2011) No evidence for increased skin cancer risk in Koreans with skin phototypes III–V treated with narrowband UVB phototherapy. *Acta. Derm. Venereol.* **91**, 40–43.
 34. Mera, K., K. Kawahara, K. Tada, K. Kawai, T. Hashiguchi, I. Maruyama and T. Kanekura (2010) ER signaling is activated to protect human HaCaT keratinocytes from ER stress induced by environmental doses of UVB. *Biochem. Biophys. Res. Commun.* **397**, 350–354.
 35. Zgheib, C., M. Hodges, J. Hu, D. P. Beason, L. J. Soslowsky, K. W. Liechty and J. Xu (2016) Mechanisms of mesenchymal stem cell correction of the impaired biomechanical properties of diabetic skin: The role of miR-29a. *Wound Repair Regen.* **24**, 237–246.
 36. Liu, P., Y. Zhu, Q. Li and B. Cheng (2020) Comprehensive analysis of differentially expressed miRNAs and mRNAs reveals that miR-181a-5p plays a key role in diabetic dermal fibroblasts. *J. Diabetes Res.* **2020**, 4581954.
 37. Li, Y. B., Q. Wu, J. Liu, Y. Z. Fan, K. F. Yu and Y. Cai (2017) Mir199a3p is involved in the pathogenesis and progression of diabetic neuropathy through downregulation of serpine2. *Mol. Med. Rep.* **16**, 2417–2424.
 38. Soonthornchai, W., P. Tangtanatakul, J. Meehansan, K. Ruchusatsawat, R. Reantragoon, N. Hirankarn and J. Wongpiyabovorn (2019) Down-regulation of miR-155 after treatment with narrow-band UVB and methotrexate associates with apoptosis of keratinocytes in psoriasis. *Asian Pac. J. Allergy Immunol.* **39**, 206–213.
 39. Fish, J. E., M. M. Santoro, S. U. Morton, S. Yu, R. F. Yeh, J. D. Wythe, K. N. Ivey, B. G. Bruneau, D. Y. Stainier and D. Srivastava (2008) Mir-126 regulates angiogenic signaling and vascular integrity. *Dev. Cell* **15**, 272–284.
 40. Jiang, B., Y. Tang, H. Wang, C. Chen, W. Yu, H. Sun, M. Duan, X. Lin and P. Liang (2020) Down-regulation of long non-coding RNA HOTAIR promotes angiogenesis via regulating miR-126/SCEL pathways in burn wound healing. *Cell Death Dis.* **11**, 61.
 41. Wu, K., Y. Yang, Y. Zhong, H. M. Ammar, P. Zhang, R. Guo, H. Liu, C. Cheng, T. M. Koroscil, Y. Chen, S. Liu and J. Bihl (2016) The effects of microvesicles on endothelial progenitor cells are compromised in type 2 diabetic patients via downregulation of the miR-126/VEGFR2 pathway. *Am. J. Physiol. Endocrinol. Metab.* **310**, E828–E837.
 42. Jansen, F., X. Yang, M. Hoelscher, A. Cattelan, T. Schmitz, S. Proebsting, D. Wenzel, S. Vosen, B. S. Franklin, B. K. Fleischmann, G. Nickenig and N. Werner (2013) Endothelial microparticle-mediated transfer of microrna-126 promotes vascular endothelial cell repair via spred1 and is abrogated in glucose-damaged endothelial microparticles. *Circulation* **128**, 2026–2038.
 43. Zhang, J., X. J. Sun, J. Chen, Z. W. Hu, L. Wang, D. M. Gu and A. P. Wang (2017) Increasing the miR-126 expression in the peripheral blood of patients with diabetic foot ulcers treated with maggot debridement therapy. *J. Diabetes Complications* **31**, 241–244.